

Article

Experimental Study on the Mechanical Properties of Xinyang Red Clay Improved by Lime and Fly Ash

Hui Tang ¹, Ziquan Yang ^{1,2,*}, Hongtao Zhu ¹ and Haoqiang Dong ¹¹ School of Civil Engineering, Xinyang College, Xinyang 464000, China² School of Civil Engineering and Architecture, Wuhan University of Technology, Wuhan 430070, China

* Correspondence: zqyxyc@163.com

Abstract: There is limited research on the utilization of lime and fly ash for improving the mechanical properties of red clay soils. This study investigates the physical and mechanical properties of modified red clay with single fly ash, single lime, and mixed cases using various experimental tests, such as direct shear tests, unconfined compression tests, etc. Scanning electron microscopy was also used to analyze the microstructure of the modified red clay. The findings indicate that the incorporation of lime and fly ash resulted in a decrease in the liquid limit, plasticity index, and maximum dry density of the modified soils, while increasing the plastic limit and optimum water content. The enhancement of lateritic soils by lime and fly ash was primarily attributed to the generation of gel substances from the active ingredients, which improved the soil microstructure and increased its strength. The case study in this paper provides a new perspective on soil improvement.

Keywords: soil improvement; limit water content test; compaction test; direct shear test; unconfined compression test



Citation: Tang, H.; Yang, Z.; Zhu, H.; Dong, H. Experimental Study on the Mechanical Properties of Xinyang Red Clay Improved by Lime and Fly Ash. *Appl. Sci.* **2023**, *13*, 6271. <https://doi.org/10.3390/app13106271>

Academic Editor: Tiago Miranda

Received: 21 April 2023

Revised: 13 May 2023

Accepted: 18 May 2023

Published: 20 May 2023



Copyright: © 2023 by the authors. Licensee MDPI, Basel, Switzerland. This article is an open access article distributed under the terms and conditions of the Creative Commons Attribution (CC BY) license (<https://creativecommons.org/licenses/by/4.0/>).

1. Introduction

Red clay is a highly plastic clay of brown-red and yellow-brown color, formed by intense weathering of carbonate rocks in a temperate and humid subtropical climate [1,2]. Its mineral composition is dominated by kaolinite, illite, and chlorite, and it is characterized by a high natural water content, a high porosity ratio, and low density [3]. As a wide range of engineering materials, such as roadbed filler and slope filling, red clay is prone to appear with a large number of cracks, expansion and contraction, and other adverse engineering characteristics in the project if it is not improved, leading to road subsidence and slope sliding [4]. The most commonly used method for improving red clay is to add lime, fly ash, cement or lime–cement, fly ash–cement, and other materials in a certain proportion [5–8]; there are also other engineering soft soil improvement methods [9,10].

At present, the research on improving engineering soft soil mainly focuses on three aspects. The first is to analyze the incorporation of different improving materials macroscopically, test the physical and mechanical property indexes through geotechnical experiments, and compare and analyze the indexes before the improvement to determine the optimal incorporation ratio of the improving materials. For example, Hosseini et al. [11] used fly ash, water glass mortar, and NaOH solution as an activator to improve highly plastic clay. Through experiments, it was found that 25% of the improving material was the most effective in improving the compressive strength of the soil. Zhang et al. [12] used jute fiber and lime to improve argillaceous soil. Jute fiber has a certain elongation, and the optimal addition amount of jute fiber is 1% based on the unconfined compressive strength and ductility of the soil. Moreira et al. [13] mixed 60% construction waste particle material into the sediment silt, and the soil load ratio, resilience modulus, and unconfined compressive strength achieved satisfactory results. Gerard et al. [14] added 8% waste concrete into silty sand and crushed it into fine material and 6% lime, which showed the maximum bearing

ratio of soil and significantly increased shear strength. Baldovino et al. [15] added 9% lime to silty soil. After curing for 180 days, the tensile strength and unconfined compressive strength of the silty soil reached the maximum. Jamsawang et al. [16] used ordinary silicate cement and fly ash to improve dredged silt. The content of ordinary silicate cement is 5% and that of fly ash is 10%, and the mechanical property reached the maximum. Atahu et al. [17] added 20% coffee shell ash to expansive soil, and the bearing capacity of the soil increased by three times. Sukmak et al. [18] used palm oil fuel ash as a precursor and mixed sodium silicate solution and sodium hydroxide solution as alkaline stimulation. Sukprasert et al. [19] used fly ash and blast furnace slag to improve silty clay, and found that the strength of the soil is affected by the interaction between soil particles, mainly from chemical bonding strength, and the optimal ratio is 20:10. Panich et al. [20] added bagasse ash and fly ash into clay to improve the clay. At the same time, a mixed sodium silicate solution and sodium hydroxide solution were added as an alkaline activator, and the appropriate dosage was 5–10%. Yaghoubi et al. [21] modified soft marine clay with fly ash and slag, and different combinations of sodium- and potassium-based liquid alkaline activators (L) were added to the soil to improve soil strength. The strength of the combination of 30% NaOH with 70% Na_2SiO_3 composite is the highest. Yaghoubi et al. [22] also improved soft clay with high water content by adding a polymer made of fly ash and fine blast furnace slag. The comparison analysis showed that when the content of polymer and cement was 20%, and the curing time was 28 days, the polymer-improved soil had higher strength and more acid-resistant properties.

The second is to analyze the failure mechanism of soil after adding the improved material. Eslami et al. [23] mixed rubber waste into clay, studied the failure mode of improved soil through an unconfined strength test, and proposed an expression to estimate the strength of improved soil. Moreira et al. [24] incorporated a certain amount of cement-modified silt with debris waste particles, and derived the correlation formula between unconfined strength and the amount of added material based on the experimental data. Ikeagwuani et al. [25] used lime and bamboo ash to improve an expansive soil, and established a polynomial model relationship between the compression index and the added improved material. Nitish et al. [26] enhanced soil properties by adding fly ash, lime sludge, and polypropylene fiber to the soil. Through a series of laboratory experiments, the results were compared and a significant improvement in the strength of the soil was found, and these admixtures had a positive effect on the stability enhancement of the clay soil.

The third is to explore the mechanism of improving engineering soil microscopically by means of scanning electron microscopy and X-ray diffraction [27]. Ramezani et al. [28] used scanning electron microscopy (SEM), X-ray diffraction (XRD), and Fourier transform infrared spectroscopy (FTIR) to evaluate the microstructure of bagasse ash, glass powder, and silica fume poorly modified graded sand. Rajabi et al. [29] used metakaolin to improve clay sand. XRD showed that the cement compound calcium silicate hydrate appeared in the improved soil, and SEM imaging showed that with the addition of metakaolin, the scattered structure of the soil changed to a flocculent structure, thus enhancing the strength of the soil. Wu et al. [30] used cement and metakaolin admixture to improve the compacted soil, and used X-ray diffraction, scanning electron microscopy, thermogravimetric analysis, and mercury injection to analyze the microstructure, showing that the addition of metakaolin increased the number of hydration products and made the distribution of microscopic pores denser. Nwonu et al. [31] synthesized polymer-modified black clay from industrial wastes. Through mineralogical identification, morphology, and element analysis, the microlevel changes of geopolymer-treated soil were defined. According to the microanalysis, this method was superior to lime. Anant et al. [32] improved expansive soil with alkali-excited fly ash, and analyzed the microstructure of untreated and treated BCS samples by SEM, XRD, and FTIR spectra, showing that the combination of soil particles and the formation of dense microstructure produced higher strength and reduced expansion and shrinkage characteristics.

However, there are few studies on the engineering mechanical properties and microstructure of red clay improved by mixed lime and fly ash. Particularly, more systematic studies on the mechanical properties and microstructure of the improved soils are needed. For this reason, a soil improvement study from the Xinyang region was conducted as a case study for analysis. In this paper, Xinyang red clay was improved by single and compound lime and fly ash, and the engineering mechanical properties of the soils were compared and analyzed under different improvement methods. Using scanning electron microscopy and X-ray diffraction, the mechanism of lime and fly ash improving red clay was analyzed microscopically, which can provide a reference for road engineering and slope engineering in areas with red clay.

2. Soil Samples and Experimental Scheme

2.1. Soil Samples

The site of the test is Shihe District, Xinyang City, near Haowan Village, Dongjiahe Town. Undisturbed soil was collected. According to the undisturbed soil sampling method, rotary excavation drilling was used to collect soil. The depth of soil sampling was 4.5–5.0 m, belonging to the Quaternary Pleistocene soil. A total of 150 kg of soil was taken, and 12 sample specimens were prepared. The collected soil samples should be wrapped with black plastic film and marked with information such as the time, place, and depth of soil collection to avoid the loss of moisture and ensure the integrity of the soil samples. The collected soil samples should be tightly wrapped with cardboard shells and tape. The box is lined with damping material, and the soil sample is packed and shipped back to the laboratory. According to the laboratory soil test, the natural water content of the original red clay is 32.5%, the density is 1.86 g/cm³, the void ratio is 1.17, the optimal water content is 20.8%, the maximum dry density is 1.76 g/cm³, the compression coefficient a_{1-2} is 0.64 MPa⁻¹, and the particle size less than 0.075 mm occupies 72.3%. X-ray fluorescence was used to test the mineral composition of the red clay. The test results are shown in Table 1.

Table 1. Mineral composition of red clay.

Mineral Composition	SiO ₂	Al ₂ O ₃	Fe ₂ O ₃	K ₂ O	Others
Mass fraction (%)	44.64	28.32	20.67	1.87	4.5

2.2. Modified Material

Improved red clay uses two materials, lime and fly ash. Quick lime is adopted, with a CaO content of 92.5%. The fly ash is grayish-brown, has spherical particles, a specific gravity of 2.71, and an effective diameter of 0.05 mm. Particles with a particle size less than 0.05 mm account for 75.6% of the total mass, and the main components, Fe₂O₃, SiO₂, and Al₂O₃, account for 83.5% of the total mass. The specific content of fly ash is shown in Table 2.

Table 2. Mineral composition of fly ash.

Mineral Composition	SiO ₂	Al ₂ O ₃	Fe ₂ O ₃	GaO	Others
Mass fraction (%)	43.21	33.86	6.43	9.63	6.87

2.3. Test Setup

Take a certain amount of red clay, after drying in the oven, use the wood hammer to break the soil block. The dry red clay soil (as shown in Figure 1) that passed through the 2 mm sieve was divided into four groups. The first group is the single lime group, adding lime by 2%, 5%, 8%, and 11%. The second group is the single fly ash group, adding fly ash by 5%, 10%, 15%, and 20%. The third group is the mixed lime–fly ash group, and the mass ratios of lime–fly ash to dry soil are 1:2:7, 1:3:6, and 1:4:5. The fourth group is the control group, without lime or fly ash. Add a certain amount of water to each soil sample plate, add lime or fly ash in the corresponding proportion, mix the soil, wrap

the soil sample plate with plastic film, and then put the soil sample plate into a constant temperature and humidity curing box for 14 days under the condition of $20 \pm 2^\circ\text{C}$ and relative humidity $> 90\%$. After the curing, take the excavated plate from the curing box in batches; first use the portable compactor to make the remodeled soil sample, and then make the sample required for the corresponding test. According to the “Standard for Geotechnical Test Methods” (BG/T50123-1999), the limitation water content test, direct shear test, unconfined compression test, compaction test, and consolidation test were carried out. The experimental items, experimental instruments, and experimental record data are shown in Table 3. According to the test results, we compared and analyzed the change law of physical and mechanical parameters of the improved soil with the additional of lime and fly ash.



Figure 1. Red clay soil sample.

Table 3. Experimental items and recorded data.

Experimental Items	Experimental Instruments	Testing Parameters
Limit water content experiment	Liquid–plastic combined tester	Plastic limit Liquid limit
Compaction experiment	Standard portable compaction instrument	Optimal water content Maximum dry density
Direct shear experiment	Strain-controlled direct shear apparatus	Cohesion Friction angle
Unconfined compression experiment	Strain-controlled unconfined pressure gauge	Unconfined compressive strength
Consolidation experiment	Fully automatic consolidation instrument	Compression coefficient

3. Test Results and Analysis

3.1. Limitation Water Content Test

The plastic limit and liquid limit of soil samples with different modified materials and different mixing amounts are tested by the liquid–plastic limit tester, and the plasticity index is calculated. The results are shown in Figure 2. The liquid limit, plastic limit, and plasticity indexes of remolded red clay are 38.4%, 20.2%, and 18.2. It can be seen from Figure 1 that the liquid–plastic limit and plasticity index of the soil mass can be improved by adding lime and fly ash individually or in combination. The liquid limit and plasticity index decreased with the increase of the proportion of lime and fly ash, while the plastic limit increased with the increase of the amount of lime and fly ash. When the lime content is 5%, the liquid limit drops to 35.5%, the plastic limit rises to 25.7%, and the plasticity index drops to 9.6. At 0–2% and 8–11%, the plastic limit, liquid limit, and plasticity index have little change. It can be seen that it is appropriate to use only lime to improve the red clay,

with a mixing amount of 5%. When the content of fly ash is 10%, the liquid limit decreases to 33.5%, the plastic limit increases to 23.5%, and the plasticity index decreases to 10. When the content of fly ash is 0–5% and 15–20%, the plastic limit, liquid limit, and plasticity index have little change. When the red clay is improved by adding lime and fly ash, the ratio of 1:2:7 is better according to the change of plastic limit, liquid limit, and plasticity index.

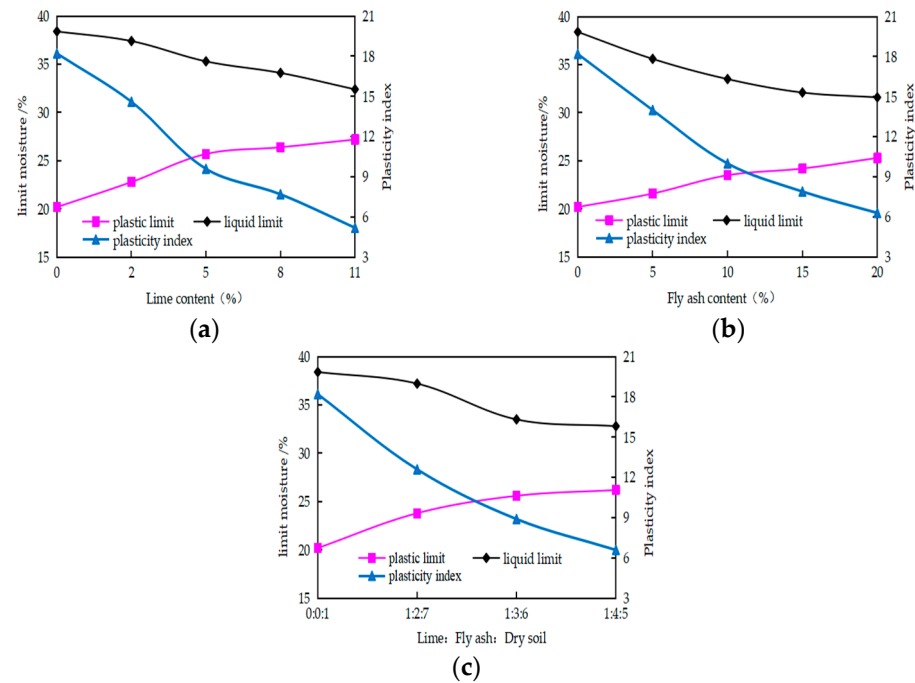


Figure 2. Change curve of limit moisture content and plasticity index with the content of modified materials: (a) single lime, (b) single fly ash, and (c) mixed lime and fly ash.

After adding lime, CaO in lime reacts with the water in red clay to generate Ca(OH)_2 , which consumes part of the free water; the Ca^{2+} , ionized from Ca(OH)_2 , displaces K^+ and Na^+ on the surface of red clay particles, reducing the thickness of the bound water film and increasing the attraction between particles. The addition of lime reduces the proportion of clay particles in the soil, reducing the hydrophilicity of the soil. After the fly ash is added, the active substances in the fly ash and the free water in the red clay will undergo hydrolysis and hydration reactions, and the active SiO_2 and Al_2O_3 will be released to generate compounds such as silicic acid, aluminic acid, and ferritic acid. The liquid limit and plasticity index of the improved red clay decreased, while the plastic limit increased.

3.2. Compaction Test

The change law of optimal water content and maximum dry density of modified soil with the addition of lime and fly ash is shown in Figure 3. As can be found from the figure, the maximum dry density of modified red clay decreases with the increase of the added lime and fly ash, but the overall decrease is small, while the optimal water content gradually increases. This is because red clay has an aggregate structure, while fly ash and lime have a granular structure. Fly ash and lime particles fill the pores between the red clay particles. In this way, the active substances in fly ash and lime, and the particles in the red clay, have an ion displacement effect. The particles of fly ash and lime are fine, the specific surface area is large, and they have strong hydrophilicity, so the optimal water content increases.

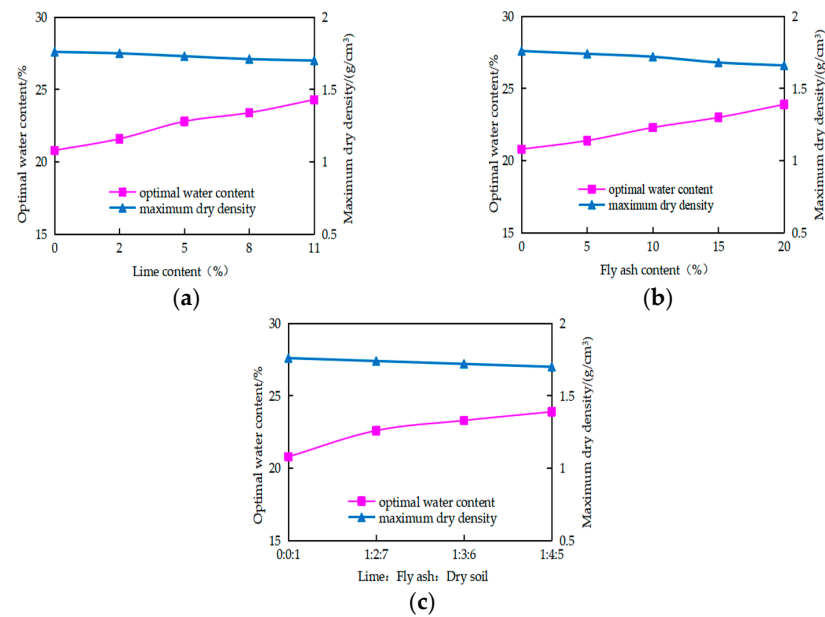


Figure 3. Compaction test results: (a) single lime, (b) single fly ash, and (c) mixed lime and fly ash.

3.3. Direct Shear Test

Three samples were installed at a time, and vertical loads of 50 kPa, 100 kPa, and 200 kPa were applied. The curve of shear strength of modified red clay with the addition of lime and fly ash under each vertical load is shown in Figure 4. The shear strength indexes of cohesion and internal friction angle are shown in Table 4. As can be seen from Figure 4, the shear strength of the modified soil is lower than that of the remolded red clay when the lime content is 2% and the fly ash content is 5%, with the vertical loads at 50 kPa and 100 kPa. The shear strength of the modified soil increases with the addition of lime and fly ash. The shear strength of the modified soil with a single lime addition of 5% reaches the maximum under each vertical load. The shear strength of the modified soil with a single lime addition is higher than that of the soil with a single fly ash addition, and then decreases with the addition of lime and fly ash. The shear strength of red clay increased with the increase of lime, fly ash, and dry soil ratio. When the ratio was 1:2:7, the shear strength reached the maximum.

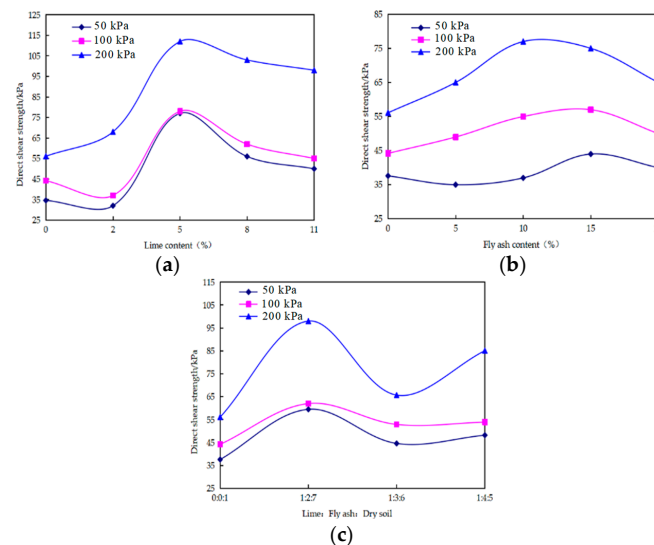


Figure 4. Curves of direct shear strength with the addition of modified materials: (a) single lime, (b) single fly ash, and (c) mixed lime and fly ash.

Table 4. Test results of shear strength index of modified red clay.

Lime Content (%)	Cohesion (kPa)	Friction Angle (°)	Fly Ash Content (%)	Cohesion (kPa)	Friction Angle (°)	Lime: Fly Ash: Dry Soil	Cohesion (kPa)	Friction Angle (°)
2	18	14	5	26	11	0:0:1	30	12.5
5	43	14	10	30	13	1:2:7	46	12.8
8	38	15	15	36	12	1:3:6	32	10.2
11	34	17	20	34	10	1:4:5	38	13

From Table 3, it can be seen that when only lime is added and the lime content is 5%, the cohesion reaches the maximum value of 43 kPa and the internal friction angle is 14°, which is 0.43 times and 0.16 times higher than the cohesion and internal friction angle of the red clay before improvement, respectively. When only fly ash is mixed and the fly ash content is 15%, the cohesion is 36 kPa at maximum and the internal friction angle is 12°; the cohesion is 0.2 times higher and the internal friction angle is 4% higher than before the improvement. When the ratio of lime: fly ash: dry soil is 1:2:7, the maximum cohesion is 46 kPa and the angle of internal friction is 12°; the cohesion of laterite increases 0.53 times compared to before improvement, and the angle of internal friction increases only 2.4%. It can be seen that the improvement of red clay with lime and fly ash has a significant effect on the shear strength index of cohesion, but has no significant effect on the internal friction angle.

After the addition of quick lime, the Ca^{2+} produced by the hydration reaction exchanges with low-price cations on the soil surface, making the binding water film on the surface of soil particles thinner, shortening the distance between soil particles, increasing the force between particles, and making the overall structure denser, which is shown as an increase in shear strength on a macro scale. However, when the proportion of lime is higher, more free water in the red clay will be consumed, which makes the thickness of the bonded water film on the surface of the soil particles smaller, and weakens the interaction between the particles. After adding a certain amount of fly ash, the generated active substance is wrapped on the surface of fly ash and red clay particles, which promotes the formation of small aggregate structure; small aggregate structure forms the large aggregate structure, cementing each other, reducing pores, increasing the interaction between aggregate structure, enhancing cohesion, and improving the shear strength of the soil to different degrees. However, when lime and fly ash are blended separately and in larger amounts, the shear strength starts to decrease; to reveal the intrinsic mechanism, more research is needed.

3.4. Unconfined Compressive Strength Test

The unconfined compressive strength of different improved red clay was tested. The variation of the unconfined compressive strength of improved red clay with different incorporation amounts of lime and fly ash is shown in Figure 5.

As can be seen from Figure 5a, the unconfined compressive strength of red clay improved by lime only increases at first with the increase of lime content, and reaches a maximum value of 2.94 MPa when the lime content is 5%, which is 2.0 times higher than that of 0% lime content, and then decreases with the further increase of lime content. As can be seen from Figure 5b, the unconfined compressive strength of red clay improved by single fly ash increases at first, and then decreases with the further increase of fly ash content. When the fly ash content is 10%, the unconfined compressive strength reaches the minimum value of 0.84 MPa, and then increases with the increase of fly ash content. When the fly ash content is 20%, the unconfined compressive strength of the improved soil reaches the maximum value of 2.24 MPa. A comparative analysis of Figure 5a,b shows that, based on the unconfined compressive strength of the improved soil, it is not difficult to see that the red clay improved more by only mixing lime rather than fly ash. As can be seen from Figure 5c, the unconfined compressive strength of the modified soil increased at first

with the soil ratio, and reached a maximum value of 2.98 MPa when the ratio is 1:2:7, and then decreased with the increase of the ratio.

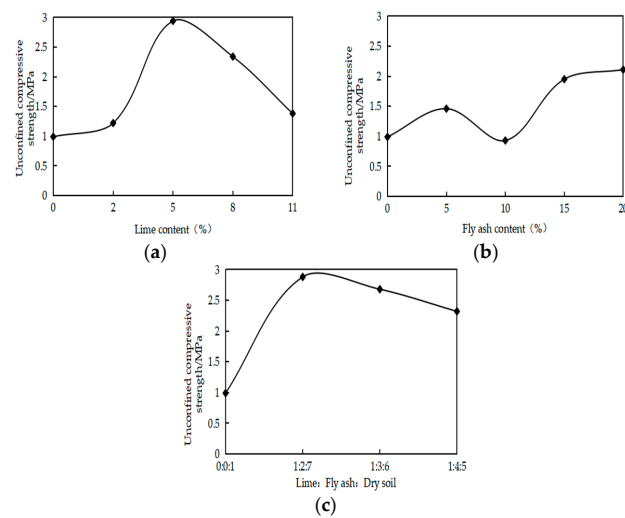


Figure 5. Curves of unconfined compressive strength with modified materials incorporated: (a) single lime, (b) single fly ash, and (c) mixed lime and fly ash.

In the test, it was found that with the increase of fly ash incorporation, the improved soil gradually showed a certain brittleness. Particularly, the soil was improved by using lime-mixed fly ash. Figure 6 shows the failure of the unconfined compression test samples with different proportions. As can be seen from Figure 6, the included angle between the failure surface and the horizontal plane of the sample increases with the increase of the proportion of lime: fly ash: dry soil, and the sample has a clear fracture surface when the ratio is 1:2:7 and 1:3:6. When the ratio is 1:4:5, after the sample reaches a certain pressure in the process of compression, it is found that slag begins to drop at both ends of the sample and gradually transfers to the middle of the sample, resulting in the local block falling and slight cracking in the middle of the sample, and the fracture surface is almost perpendicular to the major principal stress surface.

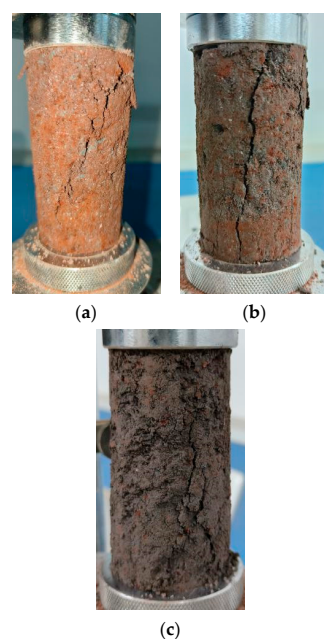


Figure 6. Failure modes of unconfined compressive test samples of modified soil with different proportions: (a) 1:2:7, (b) 1:3:6, and (c) 1:4:5.

3.5. Compression Test

Unidirectional consolidation soil is used for the unconfined compression test, and four stage loads of 50 kPa, 100 kPa, 200 kPa, and 400 kPa are applied. The corresponding void ratio is calculated according to Formula (1), and the compression coefficient a_{1-2} is calculated according to Formula (2). The variation law of the compression coefficient a_{1-2} with the incorporation amount of fly ash and lime is shown in Figure 7.

$$e_i = e_0 - \frac{s}{H_0}(1 + e_0) \quad (1)$$

where, e_i is the porosity ratio of samples under grade i load compression and stability; e_0 is initial pore ratio of sample; H_0 is initial height of sample; s is the cumulative compression value of the sample.

$$a_{1-2} = \frac{e_1 - e_2}{p_2 - p_1} \quad (2)$$

where, p_1 and p_2 are taken as 100 kPa and 200 kPa, respectively; e_1 and e_2 are void ratios under compression and stability of loads p_1 and p_2 , respectively.

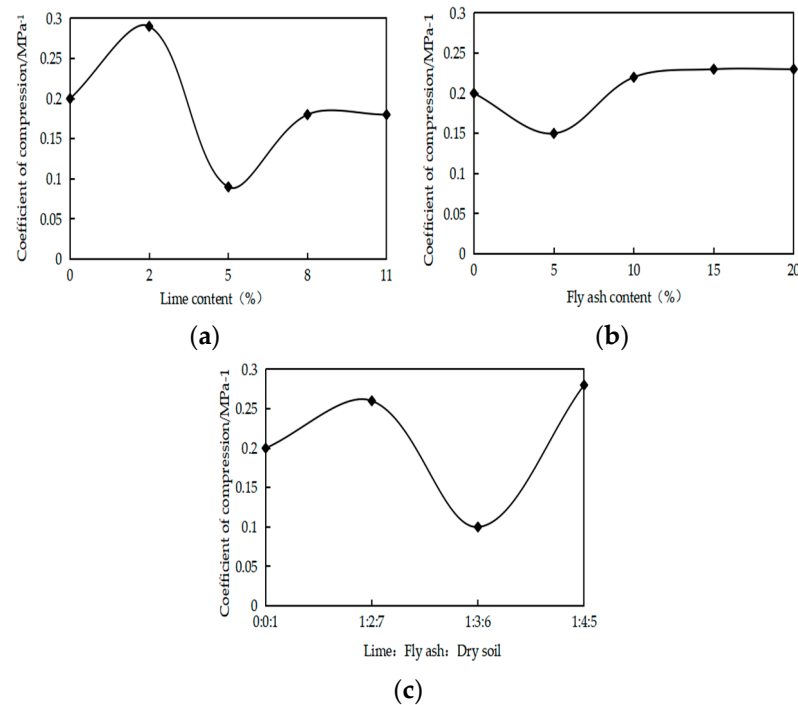


Figure 7. The compression coefficient varies with modified materials incorporated: (a) single lime, (b) single fly ash, and (c) mixed lime and fly ash.

As can be seen from Figure 7, the addition of lime and fly ash can effectively reduce the compressibility of soil. When only lime is added, the compression coefficient first decreases with the increase of lime content, and then increases. When lime content is 5%, the compression coefficient is 0.09 MPa⁻¹, indicating low compressibility. When fly ash is added, the compression coefficient of modified red clay increases with the increase of fly ash content, and then tends toward a stable value of 0.22 MPa⁻¹, indicating that the improved soil has medium compressibility. When lime and fly ash are mixed together, increasing the amount of fly ash in the mixture leads to a decrease in the compression coefficient. When the ratio is 1:3:6, the compression coefficient reaches a minimum of 0.1 MPa⁻¹. Continuing to increase the proportion of fly ash, the compression coefficient starts to increase again. The main reason is that the fly ash is mixed in a large amount, and the active ingredients in the fly ash cannot react fully, resulting in some fly ash particles

filling in the pores of the red clay. These fly ash particles is not cohesive. It is beneficial to the relative migration of soil particles, leading to the increase of the compression coefficient.

4. Microscopic Test

4.1. Sample Preparation

A ring cutter sample with an inner diameter of 61.8 mm and a height of 20 mm was made from unmodified material, and lime fly ash modified red clay in accordance with the ratio, and each ring cutter sample was divided into parts (each with a height of 10 mm). The sample was placed in the oven to dry, and then the fresh section soil of the drying soil sample was torn off with tweezers. A field emission scanning electron microscope was used. The pore distribution and filling of red clay and improved soil were observed. An X-ray diffractometer was used to test the main components of red clay and improved soil.

4.2. Microstructure Analysis of Improved Soil

A field emission scanning electron microscope was used to conduct scanning electron microscopy on the original red clay and the improved soil [27]. The microstructure is shown in Figure 8, as well as the analysis of the main components of the improved soil. Among them, (a) is red clay, (b) is 1:2:7 mixed with lime–fly ash improved soil sample, (c) is 1:3:6 mixed with lime–fly ash improved soil sample, and (d) is 1:4:5 mixed with lime–fly ash improved soil sample.

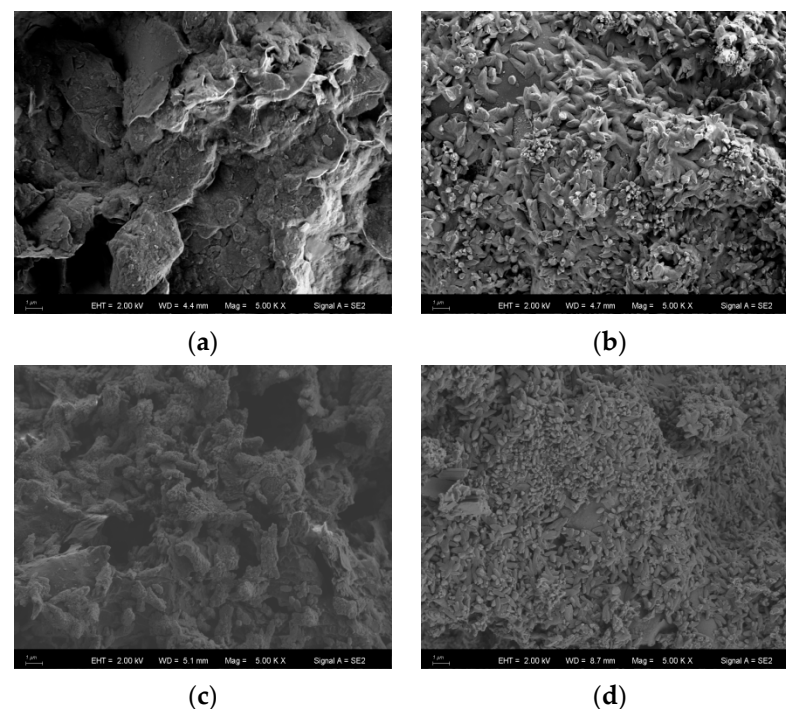


Figure 8. Remolding red clay and improving its microstructure (5000 times): (a) red clay, (b) 1:2:7, (c) 1:3:6, and (d) 1:4:5.

As can be seen from Figure 8, the particle size of red clay is small, the shape of red clay is mostly flat and irregular, and there are many small pores among the particles. The red clay is improved by adding lime and fly ash. The main reason is that the active substance CaO reacts with the free water in the red clay to produce Ca(OH)_2 , and the generated Ca(OH)_2 ionizes Ca^{2+} and $(\text{OH})^-$. When Ca^{2+} reaches a certain concentration, it replaces the low-price cations on the surface of the red clay particles, changing the electrical properties of the surface of the soil particles, thus enhancing the interparticle cohesion. At the same time, Ca(OH)_2 further reacts with the SiO_2 and Al_2O_3 in clay to produce calcium silicate hydrate (C–S–H) and calcium aluminates hydrate (C–A–H), respectively [7,8]. The

resulting calcium silicate hydrate (C–S–H) and calcium aluminate hydrate (C–A–H) have strong cementation and stable water stability. (C–S–H), (C–A–H), and $\text{Ca}(\text{OH})_2$ are covered on the surface of soil particles and filled in pores, and wrapped on the surface of soil particles. The loose particles are consolidated into small particles, and the small particles are reconsolidated into large particles to increase the internal cohesion of the soil, so as to improve the engineering characteristics of the red clay. Adding an appropriate amount of fly ash to increase the content of SiO_2 and Al_2O_3 in the improved soil promotes the hydration reaction to proceed forward, and increases the content of calcium silicate hydrate (C–S–H) and calcium aluminate hydrate (C–A–H). As a result, the particles are more fully coated, the pores are dense, the interaction between particles is stronger, and the engineering characteristics of the red clay are improved.

The comparative analysis of (b)(d) in Figure 8 shows that the surface of modified red clay particles, with a ratio of 1:2:7, is basically coated with the generated gel material and cemented together with each other. When the ratio is 1:4:5, the lime content is low, resulting in insufficient $\text{Ca}(\text{OH})_2$, high fly ash content, and a high content of SiO_2 and Al_2O_3 , which cannot react with $\text{Ca}(\text{OH})_2$ to form calcium silicate hydrate (C–S–H) and calcium aluminates hydrate (C–A–H). It can only be filled in the pores between soil particles or wrapped in gel materials, which cannot reach the goal of soil improvement. This is consistent with the results of the composition analysis of modified red clay in Figure 9, and the test results of the mechanical property index of the improved soil.

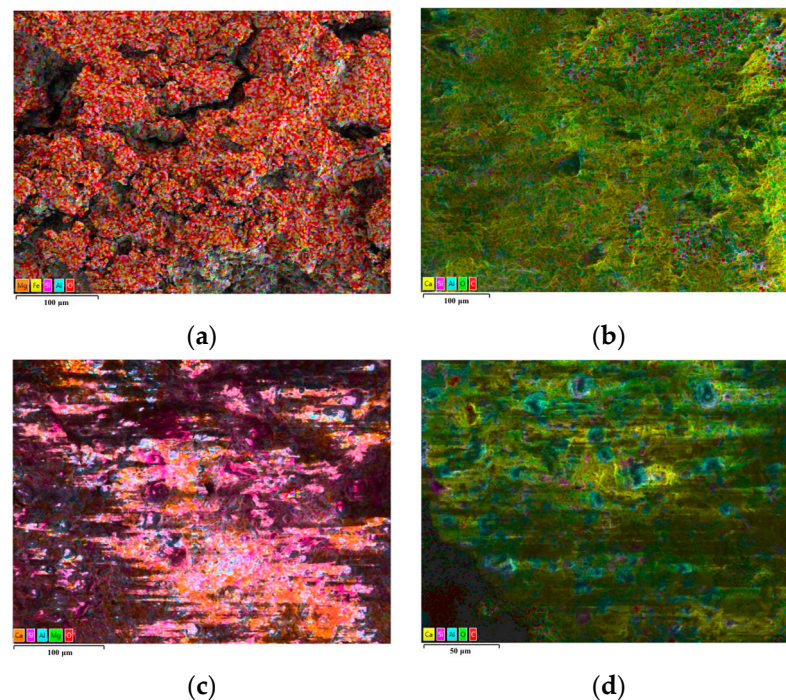


Figure 9. Energy-dispersive spectroscopy images: (a) red clay, (b) 1:2:7, (c) 1:3:6, and (d) 1:4:5.

5. Conclusions

This study focused on improving Xinyang red clay using three methods: single lime, single fly ash, and compound lime–fly ash. Various tests were conducted, including the limiting water content test, compaction test, direct shear test, unconfined compression test, compression test, and microscopic test, to analyze the physical and mechanical properties, as well as the microscopic structure of the improved red clay. The main conclusions drawn from this study are as follows:

- (1) The liquid limit, plastic index, and maximum dry density of red clay decrease with the increase of the proportion of lime and fly ash, while the plastic limit and optimal water content increase with the increase of lime and fly ash content. This suggests

that adding lime and fly ash reduces the plasticity and increases the compaction characteristics of the red clay.

- (2) The addition of lime and fly ash has a significant influence on the cohesion (c) of the shear strength index, but has no significant influence on the internal friction angle (φ). This indicates that lime and fly ash primarily affect the cohesive properties of the red clay.
- (3) When the content of lime is 5%, fly ash is 10%, and the ratio of lime to fly ash is 1:2:7, the shear strength index and unconfined compressive strength of the soil are improved, and the compressibility of the soil is reduced. This suggests that a specific combination of lime and fly ash, with appropriate proportions, yields the best results in terms of improving the mechanical properties of the red clay.
- (4) When the red clay is improved by adding lime–fly ash, the improved soil may become brittle to some extent when the fly ash content is high. Therefore, it is important to control the fly ash content appropriately, to avoid detrimental effects on the mechanical properties of the soil.
- (5) Scanning electron microscope and X-ray diffraction analysis revealed that the modified red clay particles, with a ratio of 1:2:7 of lime to fly ash, were coated with $\text{Ca}(\text{OH})_2$, calcium silicate hydrate (C–S–H), calcium aluminate hydrate (C–A–H), and other gel substances. These substances cemented the particles together, increasing the bonding force between the particles, and improving the overall structure of the red clay.

The study in this paper is still relatively shallow due to a variety of factors, such as experimental conditions. More experiments are needed in the future to explore the optimal combination of fly ash and lime content to obtain a high-performance modified Xinyang red clay. Moreover, more microstructure testing techniques need to be utilized to reveal the mechanism of the effect of different admixtures on the soil. Additionally, it is also important to characterize the natures of different phases under microstructures, and analyze the effects of phase natures on soil properties.

Author Contributions: H.T.: Writing—original draft, methodology; Z.Y.: methodology, conceptualization; H.Z.: revised manuscript, formal analysis; H.D.: formal analysis, resources. All authors have read and agreed to the published version of the manuscript.

Funding: Key Scientific and Technological Research Projects of Henan Province (232102220004).

Data Availability Statement: Some or all data during the study are available from the corresponding author by request.

Conflicts of Interest: The authors declare no conflict of interest.

References

1. Jiang, X.; Guo, J.; Yang, H.; Bao, S.; Wen, C.; Chen, J. Study on Stress–Strain Relationship of Coir Fiber-Reinforced Red Clay Based on Duncan–Chang Model. *Appl. Sci.* **2023**, *13*, 556. [\[CrossRef\]](#)
2. Zhang, Y.; Zuo, S.; Li, R.Y.M.; Mo, Y.; Yang, G.; Zhang, M. Experimental study on the mechanical properties of Guiyang red clay considering the meso micro damage mechanism and stress path. *Sci. Rep.* **2020**, *10*, 17449. [\[CrossRef\]](#) [\[PubMed\]](#)
3. Xiang, P.; Wei, G.; Zhang, S.; Cui, Y.; Guo, H. Model Test on the Influence of Surcharge, Unloading and Excavation of Soft Clay Soils on Shield Tunnels. *Symmetry* **2021**, *13*, 2020. [\[CrossRef\]](#)
4. Song, Y.; Geng, Y.; Dong, S.; Ding, S.; Xu, K.; Yan, R.; Liu, F. Study on Mechanical Properties and Microstructure of Basalt Fiber-Modified Red Clay. *Sustainability* **2023**, *15*, 4411. [\[CrossRef\]](#)
5. Dhar, S.; Hussain, M. The strength and microstructural behavior of lime stabilized subgrade soil in road construction. *Int. J. Geotech. Eng.* **2021**, *15*, 471–483. [\[CrossRef\]](#)
6. Mohamed, A.A.M.S.; Yuan, J.; Al-Ajamee, M.; Dong, Y.; Ren, Y.; Hakuzweyezu, T. Improvement of expansive soil characteristics stabilized with sawdust ash, high calcium fly ash and cement. *Case Stud. Constr. Mater.* **2023**, *18*, e01894. [\[CrossRef\]](#)
7. Barman, D.; Dash, S.K. Stabilization of expansive soils using chemical additives: A review. *J. Rock Mech. Geotech. Eng.* **2022**, *14*, 1319–1342. [\[CrossRef\]](#)
8. Abdullah, H.H.; Shahin, M.A.; Walske, M.L. Review of Fly-Ash-Based Geopolymers for Soil Stabilisation with Special Reference to Clay. *Geosciences* **2020**, *10*, 249. [\[CrossRef\]](#)

9. Tajaddini, A.; Saberian, M.; Kamalzadeh Sirchi, V.; Li, J.; Maqsood, T. Improvement of mechanical strength of low-plasticity clay soil using geopolymer-based materials synthesized from glass powder and copper slag. *Case Stud. Constr. Mater.* **2023**, *18*, e01820. [\[CrossRef\]](#)
10. Ho, L.S.; Nakarai, K.; Duc, M.; Kouby, A.L.; Maachi, A.; Sasaki, T. Analysis of strength development in cement-treated soils under different curing conditions through microstructural and chemical investigations. *Constr. Build. Mater.* **2018**, *166*, 634–646. [\[CrossRef\]](#)
11. Hosseini, S.; Brake, N.A.; Nikookar, M.; Günaydin-Şen, Ö.; Snyder, H.A. Enhanced strength and microstructure of dredged clay sediment-fly ash geopolymer by mechanochemical activation. *Constr. Build. Mater.* **2021**, *301*, 123984. [\[CrossRef\]](#)
12. Zhang, J.; Deng, A.; Jaksa, M. Enhancing mechanical behavior of micaceous soil with jute fibers and lime additives. *J. Rock Mech. Geotech. Eng.* **2021**, *13*, 1093–1100. [\[CrossRef\]](#)
13. Moreira, E.B.; Baldovino, J.d.J.A.; Luis dos Santos Izzo, R.; Rose, J.L. Impact of Sustainable Granular Materials on the Behavior Sedimentary Silt for Road Application. *Geotech. Geol. Eng.* **2020**, *38*, 917–933. [\[CrossRef\]](#)
14. Banzibaganye, G.; Twagirimana, E.; Kumaran, G.S. Strength Enhancement of Silty Sand Soil Subgrade of Highway Pavement Using Lime and Fines from Demolished Concrete Wastes. *Int. J. Eng. Res. Afr.* **2018**, *36*, 74–84. [\[CrossRef\]](#)
15. Baldovino Jair, A.; Moreira Ecclesielter, B.; Izzo, R.L.D.S.; Rose Juliana, L. Empirical Relationships with Unconfined Compressive Strength and Split Tensile Strength for the Long Term of a Lime-Treated Silty Soil. *J. Mater. Civ. Eng.* **2018**, *30*, 06018008. [\[CrossRef\]](#)
16. Jamsawang, P.; Charoensil, S.; Namjan, T.; Jongpradist, P.; Likitlersuang, S. Mechanical and microstructural properties of dredged sediments treated with cement and fly ash for use as road materials. *Road Mater. Pavement Des.* **2021**, *22*, 2498–2522. [\[CrossRef\]](#)
17. Atahu, M.K.; Saathoff, F.; Gebissa, A. Strength and compressibility behaviors of expansive soil treated with coffee husk ash. *J. Rock Mech. Geotech. Eng.* **2019**, *11*, 337–348. [\[CrossRef\]](#)
18. Sukmak, P.; Sukmak, G.; Horpibulsuk, S.; Setkit, M.; Kassawat, S.; Arulrajah, A. Palm oil fuel ash-soft soil geopolymer for subgrade applications: Strength and microstructural evaluation. *Road Mater. Pavement Des.* **2019**, *20*, 110–131. [\[CrossRef\]](#)
19. Sukprasert, S.; Hoy, M.; Horpibulsuk, S.; Arulrajah, A.; Rashid, A.S.A.; Nazir, R. Fly ash based geopolymer stabilisation of silty clay/blast furnace slag for subgrade applications. *Road Mater. Pavement Des.* **2021**, *22*, 357–371. [\[CrossRef\]](#)
20. Panich, V.; Suksun, H.; Chairat, T. Bagasse ash-fly ash-geopolymer-treated soft Bangkok clay as subgrade material. *Environ. Geotech.* **2019**, *40*, 1–8. [\[CrossRef\]](#)
21. Yaghoubi, M.; Arulrajah, A.; Disfani, M.M.; Horpibulsuk, S.; Bo, M.W.; Darmawan, S. Effects of industrial by-product based geopolymers on the strength development of a soft soil. *Soils Found.* **2018**, *58*, 716–728. [\[CrossRef\]](#)
22. Yaghoubi, M.; Arulrajah, A.; Horpibulsuk, S. Engineering Behaviour of a Geopolymer-stabilised High-water Content Soft Clay. *Int. J. Geosynth. Ground Eng.* **2022**, *8*, 45. [\[CrossRef\]](#)
23. Eslami, A.; Akbarimehr, D. Failure analysis of clay soil-rubber waste mixture as a sustainable construction material. *Constr. Build. Mater.* **2021**, *310*, 125274. [\[CrossRef\]](#)
24. Moreira, E.B.; Baldovino, J.A.; Rose, J.L.; Luis dos Santos Izzo, R. Effects of porosity, dry unit weight, cement content and void/cement ratio on unconfined compressive strength of roof tile waste-silty soil mixtures. *J. Rock Mech. Geotech. Eng.* **2019**, *11*, 369–378. [\[CrossRef\]](#)
25. Ikeagwuani, C.C.; Nwonu, D.C. Resilient Modulus of Lime-Bamboo Ash Stabilized Subgrade Soil with Different Compactive Energy. *Geotech. Geol. Eng.* **2019**, *37*, 3557–3565. [\[CrossRef\]](#)
26. Kumar Sharma, N. Utilization of fly ash, lime sludge and polypropylene fiber as stabilizers to enhance soil properties. *Mater. Today Proc.* **2022**, *65*, 988–994. [\[CrossRef\]](#)
27. Ural, N. The significance of scanning electron microscopy (SEM) analysis on the microstructure of improved clay: An overview. *Open Geosci.* **2021**, *13*, 197–218. [\[CrossRef\]](#)
28. Ramezani Seyed, J.; Toufigh Mohammad, M.; Toufigh, V. Utilization of Glass Powder and Silica Fume in Sugarcane Bagasse Ash-Based Geopolymer for Soil Stabilization. *J. Mater. Civ. Eng.* **2023**, *35*, 04023042. [\[CrossRef\]](#)
29. Rajabi, A.M.; Hamrahi, Z. An experimental study on the influence of metakaolin on mechanical properties of a clayey sand. *Bull. Eng. Geol. Environ.* **2021**, *80*, 7921–7932. [\[CrossRef\]](#)
30. Wu, Z.; Deng, Y.; Liu, S.; Liu, Q.; Chen, Y.; Zha, F. Strength and micro-structure evolution of compacted soils modified by admixtures of cement and metakaolin. *Appl. Clay Sci.* **2016**, *127*, 44–51. [\[CrossRef\]](#)
31. Nwonu, D.C.; Mama, C.N. Delineating the Aptness of Improved Geomaterial Strength for Ground Improvement Through Microstructure and Cluster Analysis. *Indian Geotech. J.* **2021**, *51*, 1151–1165. [\[CrossRef\]](#)
32. Murmu, A.L.; Jain, A.; Patel, A. Mechanical Properties of Alkali Activated Fly Ash Geopolymer Stabilized Expansive Clay. *KSCE J. Civ. Eng.* **2019**, *23*, 3875–3888. [\[CrossRef\]](#)

Disclaimer/Publisher's Note: The statements, opinions and data contained in all publications are solely those of the individual author(s) and contributor(s) and not of MDPI and/or the editor(s). MDPI and/or the editor(s) disclaim responsibility for any injury to people or property resulting from any ideas, methods, instructions or products referred to in the content.